

Jan Dutkiewicz<sup>1\*</sup>, Magdalena Szutkowska<sup>2</sup>, Wojciech Leśniewski<sup>3</sup>, Piotr Wieliczko<sup>3</sup>, Andrzej Pieczara<sup>4</sup>, Łukasz Rogal<sup>1</sup>

<sup>1</sup>Polish Academy of Sciences, Institute of Metallurgy and Materials Science, ul. Reymonta 25, 30-059 Krakow, Poland

<sup>2</sup>Institute of Advanced Technologies (IOS), ul. Wrocławska 37a, 30-011 Krakow, Poland

<sup>3</sup>Foundry Research Institute, ul. Zakopiańska 73, 30-418 Krakow, Poland

<sup>4</sup>Gonar Company, ul. Obroki 109, 40-833 Katowice, Poland

\*Corresponding author. E-mail: j.dutkiewicz@imim.pl

Received (Otrzymano) 9.04.2014

## THE EFFECT OF TiC ON STRUCTURE AND HARDNESS OF WC-Co COMPOSITES PREPARED USING VARIOUS CONSOLIDATION METHODS

The additions of 5÷10 wt.% TiC to WC-Co industrial composites substituting WC were consolidated using either the Hot Isostatic Pressing (HIP) method at the temperature of 1320°C and pressure of 250 MPa, or using the Spark Plasma Sintering (SPS) method. The latter samples show a hardness increase from 1050 HV (without TiC) up to 1330 HV at 5% TiC. A larger addition of 10% TiC allows one to obtain a similar hardness increase as in the case of the 5% addition. A higher hardness of 1570 HV was observed for samples consolidated using HIP, which can be explained by the higher consolidation pressure of 1500 bars and temperature of 1350°C leading to a lower porosity. The crack formation behavior allowed the authors to determine the fracture toughness,  $K_{IC}$ , in the range of 10.9÷11.2 MPam<sup>1/2</sup> for the samples containing 0÷10% TiC. Three phases were identified using the X-ray diffraction method, as well as scanning and transmission electron microscopy. The major identified phase is WC particles separated by a narrow layer of Co and are accompanied by single particles of TiC. It indicates that TiC do not form a common solid solution with WC as also confirmed by EDS chemical analysis, which was suggested in literature.

**Keywords:** cemented WC-TiC-Co carbides, HIP and SPS consolidation, hardness and fracture toughness measurements

## WPLYW DODATKU TiC NA STRUKTURĘ I WŁASNOŚCI KOMPOZYTÓW WC-Co WYKONANYCH Z UŻYCIEM RÓŻNYCH METOD KONSOLIDACJI

Zastosowano dodatki 5÷10% mas. do kompozytów przemysłowych WC-Co, co pozwoliło na zwiększenie ich twardości od HV<sub>30</sub> = 1050 do 1330 HV przy zawartości 5% TiC konsolidowanych przy użyciu metody zgrzewania impulsowo-plazmowego (SPS). Podobny wzrost twardości osiągnięto przy zastosowaniu dodatku 10% TiC. Pomiary odporności na pękanie metodą pęknięć przy odciskach Vickersa pozwoliły na stwierdzenie minimalnego spadku odporności z zastosowaniem dodatku TiC z 11,2 do 10,9 MPam<sup>1/2</sup>. Stosując metodę prasowania izostatycznego HIP przy ciśnieniu 1500 barów w temperaturze 1350°C, uzyskano większy przyrost twardości do 1570 HV przypuszczalnie z uwagi na uzyskaną niższą porowatość. Zidentyfikowano, stosując metody dyfrakcji rentgenowskiej i analitycznej mikroskopii elektronowej skaningowej i transmisyjnej w spiekanych obiekta metodami próbkach, trzy podstawowe fazy, a podstawową WC otoczoną cienką warstwą Co i dodatkowo pojedyncze wydzielenia TiC. Nie stwierdzono reakcji WC i TiC, co było sugerowane w literaturze, a co potwierdzono metodami mikroanalizy i dyfrakcji rentgenowskiej.

**Słowa kluczowe:** spiekane węgliki WC-TiC-Co, konsolidacja metodami SPS i HIP, pomiary twardości i odporności na pękanie

## INTRODUCTION

WC-Co hard composites are materials of significant importance for cutting, mining and chipless forming tools, as well as for high performance construction and wear parts [1, 2]. Various methods are used to improve the properties of such composites. One of them is component nanocrystallization [3-5] which is considered as an important branch of nanocrystalline materials. By combining high hardness and high toughness, they are expected to be widely applicable in industrial fields. Nanostructured WC-Co cemented carbides with a mean grain size of 250 nm were produced. The material

exhibits a high hardness of 93.6 HRA, which exceeds 1000 HV, about 50% more than conventional WC-Co composites [5]. Nanocrystalline composites attain a transverse rupture strength of 2746 MPa [5]. Another possibility used to strengthen WC-Co composites was the application of diamond coated plasma sintered composites [6]. The tungsten-coated diamond is chemically bonded with the WC-Co cemented carbide matrix, shows no reaction products between the diamond and the matrix, and the transitional zone demonstrates that the diamond matches the matrix very well. Another

possibility used was the application of carbon nanotubes when the strengthening and bonding role of carbon nanotubes occurred in the nano-WC-Co matrix, in the spark plasma sintered samples [7]. The effect of the addition of c-BN to WC-Co composites was investigated in [8]. The sintering behavior and mechanical properties of WC-Co and WC-Co-cBN composites sintered by SPS were investigated. Almost full densification of the WC-Co-cBN powders was achieved by SPS.

According to XRD and SEM analysis, there was no indication that cBN transformed to hBN. The addition of 25 vol.% cBN significantly increased the mechanical and thermal properties of the material. Ultrafine WC-Ni-VC-TiC cemented carbides with different amounts of cubic boron nitride (cBN) were applied in composites fabricated by spark plasma sintering [9]. When the fraction of cBN increased from 0 up to 50 vol.%, the hardness of the samples increased from 2100 to 3200 HV, but the flexural strength decreased from 1950 to 1250 MPa.

Titanium carbide, with a very high melting temperature of 3067°C [10], has excellent properties such as high hardness, good high-temperature strength, and good corrosion resistance. Additionally, no detrimental new phase is formed except that W diffuses into the TiC lattice to form a (Ti,W)C solid solution according to the TiC-W binary alloy diagram [11]. Partial replacement of WC by cubic TiC improved the high-temperature strength, however, no effect on the mechanical properties was investigated [12]. In the present study, the addition of various amounts of TiC up to 10 wt.% substituting WC was applied in WC-Co composites. The composites were consolidated using either SPS, uniaxial hot pressing or the HIP method. The hardness of the composites was tested and in addition the microstructure was studied using optical, scanning and transmission electron microscopy (TEM).

## EXPERIMENTAL METHOD

Table 1 shows the chemical composition of the investigated WC-Co mixtures used for the preparation of hard composites. One can see that the first 2 contain about 14 wt.% Co, while the third one only 11 wt.% Co. The content of the other elements is below 0.3% (chromium) and the other below 0.1 wt.%. The YK15.6 mixture was delivered by the Chinese producer Chongyi Zhangyuan Tungsten Co. Ltd and the other two by the German Burhaun company.

SEM micrographs of the delivered WC-Co powder mixtures are shown in Figure 1. One can see that the size of the powders varies between 0.5–5µm. Measurements using Shimadzu type SA-CP3 allowed the authors to determine the mean size of the YK15.6 mixture as 3.75 µm, that of B30/1 3.57 µm and that of B30/2 2.44 µm. They are considered optimal for the produced hard products.

TABLE 1. Chemical composition of the investigated WC-Co mixtures

TABELA 1. Skład chemiczny badanych mieszanek WC-Co

Symbol	Elements								
	WC	Co	Fe	Ti	Mo	Nb	Ni	Cr	V
YK15.6	85.77	13.9 (14.9)	0.092	0.043	0	0.013	0.082	0.305	0
B30/1	84.18	14.47 (19.0)	0.108	0.054	0	0.021	0.243	0.36	0
B30/2	89.00	11.00 (12.5)	-	-	-	-	-	-	-

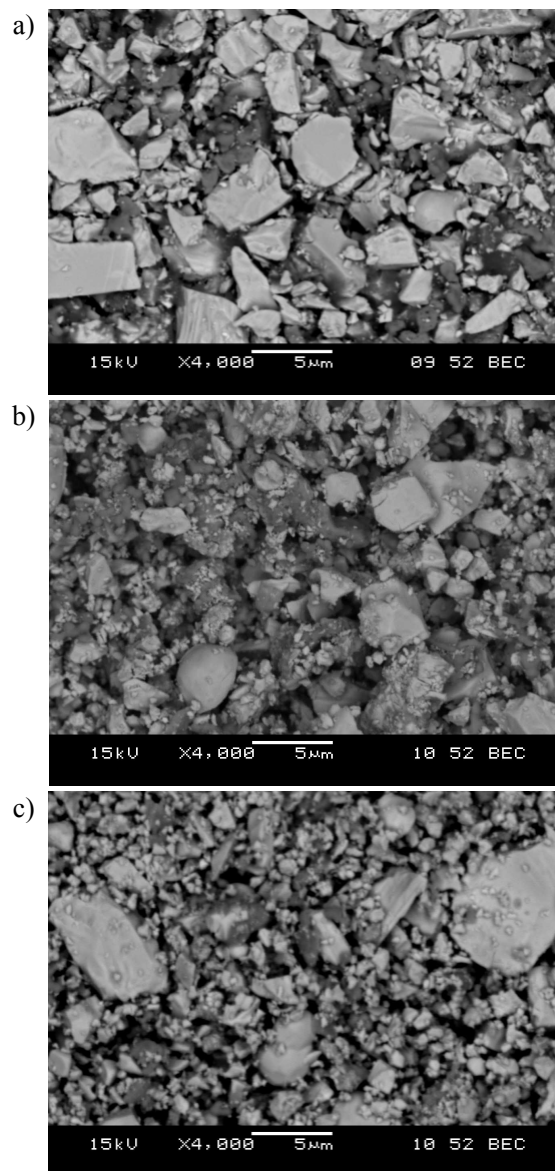


Fig. 1. SEM micrographs of delivered powder mixtures: a) YK15.6, b) B30/1, c) B30/2

Rys. 1. Mikrostruktura SEM dostarczonych mieszanek: a) YK15.6, b) B30/1, c) B30/2

The structure of the consolidated samples was studied using a Philips CM20 transmission electron microscope (TEM), scanning electron microscope FEI equipped EDS detector, Leica optical microscope equipped with QUIN quantitative image analysis, and

X-ray diffractometer Philips PW1840 using monochromatic Cu-K $\alpha$  radiation.

Part of the samples was consolidated using Spark Plasma Sintering (SPS) using HPD05 equipment at a pressure of 50 MPa and temperatures in the range of 1200–1300°C. The other part was consolidated using Hot Isostatic Pressing (HIP) using a pressure of 1500 bars and a temperature of 1350°C. The samples were placed in titanium containers, then separated by elastic graphite foil from the titanium in order to prevent a chemical reaction between the composite and the die. Afterwards, the titanium containers were welded to avoid interaction with gas. The change of the process parameters such as temperature measured in various places of the consolidated sample C1 and C3 (showing no marked differences) and pressure during consolidation using HIP are presented in Figure 2. One can see that the consolidation process using HIP took nearly 7 hours, however, the samples were kept at maximum pressure and temperature only for 1 hour.

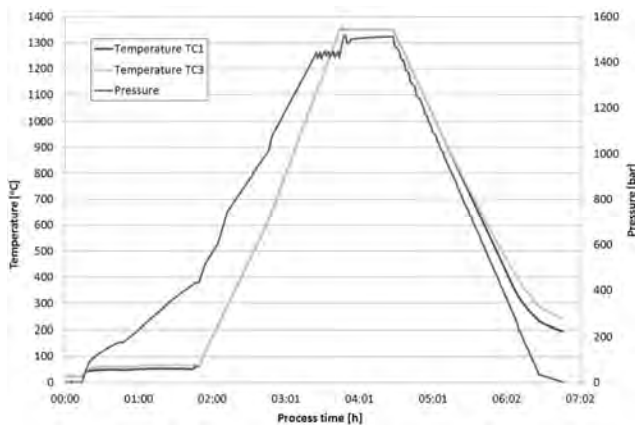


Fig. 2. Change of HIP process parameters during consolidation of investigated WC-Co + TiC composites

Rys. 2. Zmiana parametrów procesu HIP podczas spiekania próbek kompozytów WC-Co + TiC

## RESULTS AND DISCUSSION

Figure 3 shows the results of the change of density and Young's modulus in relation to SPS sintering temperature of the YK15 mixture. By conducting sintering at 1200°C, too low properties were obtained such as hardness below 500 HV and density 12.6 g/cm<sup>3</sup>, therefore higher temperatures were applied and at the temperature near 1300°C, the highest hardness and apparent density were observed. In the temperature range from 1250 to 1290°C, similar properties were obtained as can be seen in Figure 3 - about 1200 HV<sub>30</sub>, Young's modulus in the range of 559–586 GPa and apparent density in the range of 14.28–14.55 g/cm<sup>3</sup>.

Figure 4 shows the SEM micrograph from the YK15 sample consolidated using the SPS method at 1300°C. One can see the polygon shape of the WC carbides visible as bright areas about the size of several micrometers surrounded by a darker cobalt binder. Ta-

ble 3 shows Vickers hardness HV<sub>30</sub>, the apparent density and Young's modulus for WC-Co and indentation fracture toughness of the WC-Co-TiC composites prepared using various methods. One can see that the hardness increases with an increasing TiC content in the samples consolidated using the SPS method, while the samples consolidated using HIP were even harder with the same TiC content.

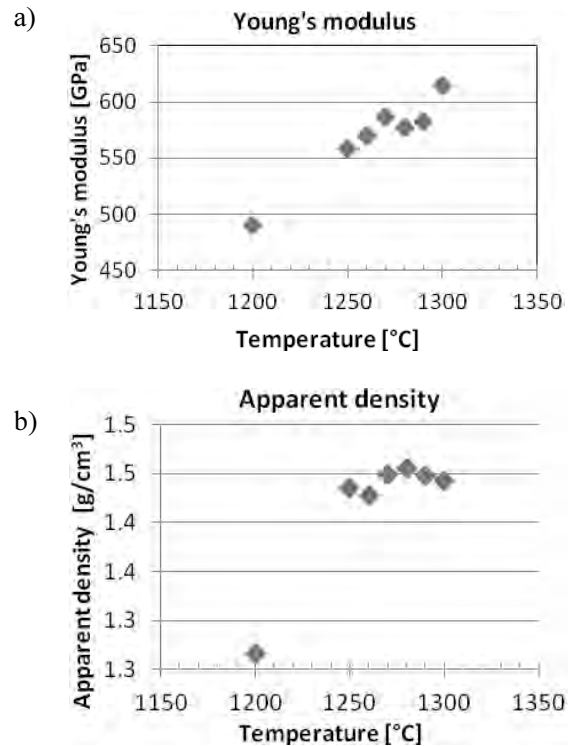


Fig. 3. Relationship of Young's modulus versus SPS sintering temperature (a) and relationship of density versus SPS sintering temperature (b)

Rys. 3. Zmiana wielkości modułu Younga próbek spiekanych metodą SPS w zależności od temperatury spiekania (a) i zależność uzyskanej gęstości od temperatury spiekania (b)

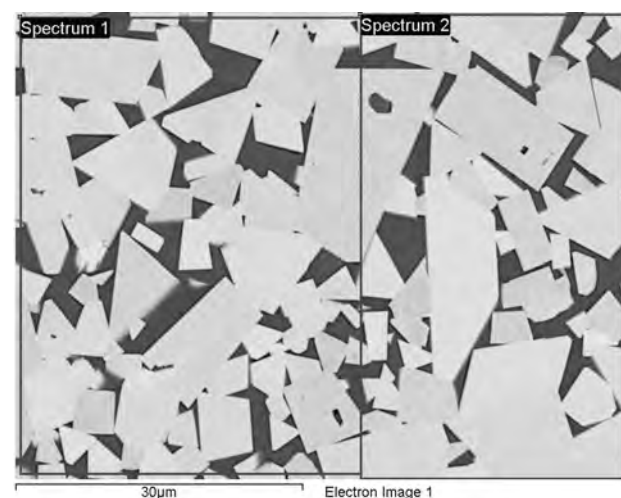


Fig. 4. SEM microstructure of SPS method sintered YK15 sample at 1300°C

Rys. 4. Mikrostruktura SEM próbki YK15 spiekanej metodą SPS w temperaturze 1300°C

TABLE 2. Vickers hardness HV30, apparent density and Young’s modulus and indentation fracture toughness of WC-Co-TiC composites prepared using various methods

TABELA 2. Twardość Vickersa HV30, gęstość pozorną, moduł Younga i odporność na pękanie mierzona długością pęknięć przy pomiarach twardości kompozytów WC-Co wytworzonych różnymi metodami

Sample	Apparent density $\rho$ [g/cm <sup>3</sup> ]	Average Vickers hardness HV30	Young’s modulus $E$ [GPa]	Poisson’s ratio $\nu$	Indentation fracture toughness $K_{IC(HV)}$ [MPam <sup>1/2</sup> ]
Gonar reference HIP		1041			
YK15.6+10 wt.% TiC-SPS	11.80	1341	478	0.21	11.2
B30/2+5 wt.% TiC-SPS	12.17	1330	466	0.21	10.82
B30 + 5 wt.% TiC HIP		1574			
B30/2+10 wt.% TiC SPS	11.38	1426	462	0.22	10.90

It is also important that the fracture toughness,  $K_{IC}$ , only insignificantly decreases with TiC addition, however, the decrease is very small as compared with the large hardness increase. Figure 5 shows X-ray diffraction curves obtained from samples B30 containing 5% and 10% TiC consolidated using the HIP process. One can distinguish 3 basic phases: WC of the highest peak intensities due to its highest fraction, then Co and TiC with increasing peak intensity when its fraction increases from 5 to 10 wt.%. No intermediate phases reported before [11] can be seen.

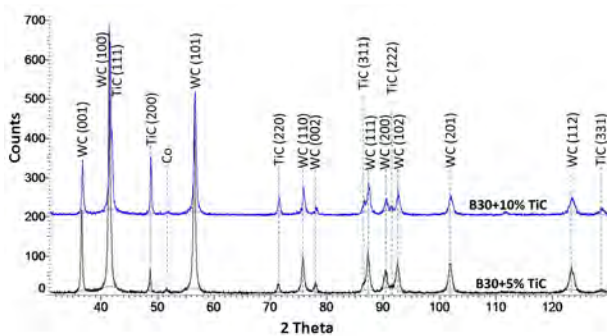


Fig. 5. X-ray diffraction of sample consolidated by HIP B30 + 5% TiC and B30 + 10% TiC

Rys.5. Dyfrakcja rentgenowska próbki spiekanej metodą HIP B30 + 5% TiC i B30 + 10% TiC

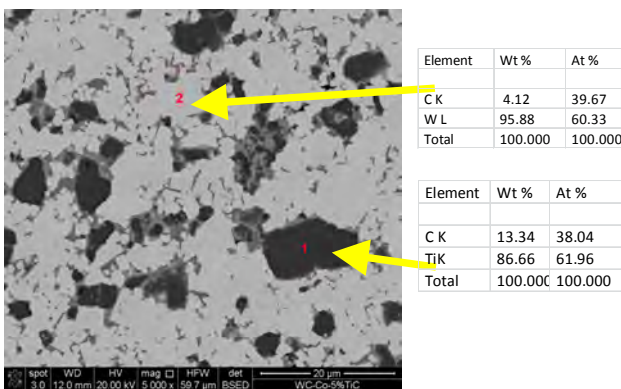


Fig. 6. SEM micrograph of WC-Co-5% TiC sample consolidated by HIP and results from EDS chemical analysis from points marked 1 and 2

Rys. 6. Mikrostruktura SEM próbki B30 WC-Co z dodatkiem 5% TiC spiekanej metodą HIP i wyniki analizy EDS dla punktów oznaczonych 1 i 2

Figure 6 confirms the results of X-ray diffraction since 3 phases can be clearly distinguished. Visible as bright areas, the WC phase of a polygon shape and size between 2÷10  $\mu\text{m}$  is surrounded by a cobalt binder visible as grey since it has a lower atomic number than W. Single TiC grains visible as dark areas were confirmed by EDS X-ray microanalysis at marked points 1 and 2 allowing the identification of WC and TiC phases without any other elemental additions indicating no reaction or solid solution between the sintered elements. The average size of the WC carbides is smaller than that shown in the samples consolidated using the SPS method, which might be one of reasons for the higher hardness of the samples consolidated using HIP. The SEM microstructure of the WC-Co sample containing an addition of 10% TiC consolidated using the HIP method is shown in Figure 7. One can see a similar range of size of carbide particles as that in the sample containing 5% TiC shown in Figure 6. The distribution of both types of carbide particles is homogeneous, however, TiC seem to be often present in colonies surrounded by a binder.

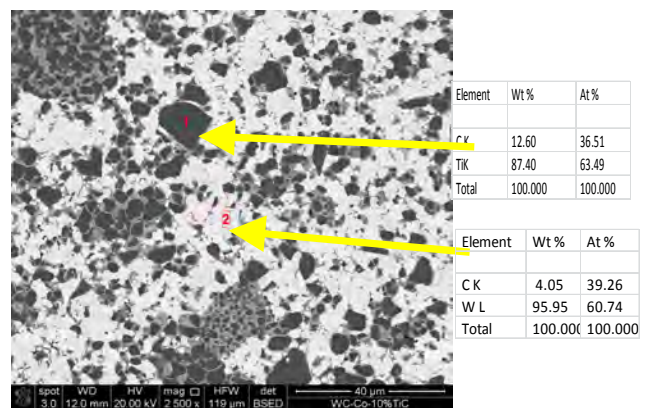


Fig. 7. SEM micrograph of WC-Co-10 wt.% TiC sample consolidated by HIP and results from EDS chemical analysis from points marked 1 and 2

Rys. 7. Mikrostruktura SEM próbki B30 WC-Co z dodatkiem 10% mas. TiC spiekanej metodą HIP i wyniki analizy EDS dla punktów oznaczonych 1 i 2

Transmission electron microscopy confirms the SEM and the X-ray diffraction data. One can see in Figure 8 relatively clean phase boundaries, where no

intermediate phases were formed at the interfaces in spite of the high process temperature. The crack formed inside the TiC phase was formed most probably during the thin foil preparation process by ion milling. Electron diffraction confirms the presence of a [012] zone axis of TiC as the central grey phase attached to WC on the right side, (appearing as very dark due to high electron absorption) of the zone axis  $[-3210]$  of the hexagonal WC carbide. The zone axes were identified based on the reflection distances and their angles showing good agreement, which allows one to be quite certain concerning the identification results. Within the TiC particle, quite a few dislocations can be clearly observed which were likely formed during the HIP process.

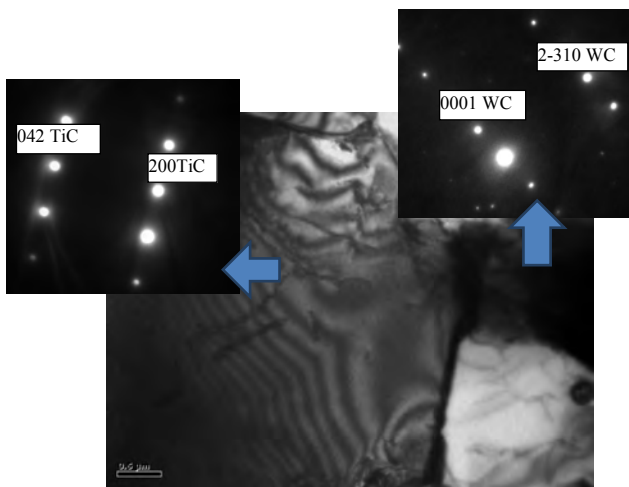


Fig. 8. TEM micrograph of WC-Co-TiC 10 wt.%. On upper left electron diffraction from TiC from the central grey part at [012] zone axis and on right diffraction from WC (dark part) at  $[-3210]$  zone axis

Rys. 8. Mikrostruktura TEM kompozytu B30 WC-Co+10% mas. TiC. Z lewej strony dyfrakcja z centralnej szarej cząstki TiC o osi pasa [0-12], a po prawej z ciemnej cząstki WC o osi pasa  $[-3210]$

## CONCLUSIONS

The application of 5÷10 wt.% TiC in WC-Co industrial composites allowed the authors to increase the hardness of the consolidated samples from  $HV_{30} = 1050$  up to  $1330 HV_{30}$  for the samples with 5 wt.% TiC consolidated using the SPS method and 1574 for the HIP consolidation. The samples with 10% TiC did not show a significant hardness increase. The crack formation along the diagonal of the indentation allowed the authors to determine the indentation fracture toughness,  $K_{IC}$ , in the range of  $10.9\div 11.2 MPam^{1/2}$  for the samples containing 0÷10 wt.% TiC. The higher hardness of the samples consolidated using HIP can be explained by finer WC particles and lower porosity due to a higher consolidation pressure. The microstructure studies show a very low porosity of samples confirming the density studies. Three phases were identified: hexago-

nal WC particles surrounded by a narrow layer of Co binder and single particles of TiC often gathered in colonies also surrounded by a binder. The microanalysis and X-ray diffraction confirmed that TiC does not form a solid solution or intermediate phases with WC. Dislocations were identified within the TiC and WC phases resulting from high pressure HIP consolidation.

## Acknowledgements

The authors are grateful for the financial support of NCBiR for experimental studies in the project GONAR: INNNOTECH-K2/IN2/20/181917/NCBR/13.

## REFERENCES

- [1] Cha S.I., Hong S.H., Ha G.H., Kim B.K., Microstructure and mechanical properties of nanocrystalline WC-10Co cemented carbides, *Scripta Materialia* 2001, 44, 1535-1539.
- [2] Gille G., Bredthauer J., Gries B., Mende B., Heinrich W., Advanced and new grades of WC and binder powder - their properties and application, *Int. J. Refract. Met. Hard Mater.* 2000, 18, 87-102.
- [3] Berger S., Porat R., Rosen R., Nanocrystalline materials: A study of WC-based hard metals, *Progress in Materials Science* 1997, 42, 311-320.
- [4] Sommer M., Schubert W.-D., Zobetz E., Warbichler P., On the formation of very large WC crystals during sintering of ultrafine WC-Co alloys, *Int. J. of Refract. Met. Hard Mater.* 2002, 20, 41-50.
- [5] Sun Jianfei, Zhang Faming, Shen Jun, Characterizations of ball-milled nanocrystalline WC-Co composite powders and subsequently rapid hot pressing sintered cermets, *Materials Letters* 2003, 57, 3140-3148.
- [6] Shi Xiaoliang, Shao Gangqin, Duan Xinglong, Yuan Runzhang, Study on the diamond/ultrafine WC-Co cermets interface formed in a SPS consolidated composite, *Rare Metals* 2006, 25, 2, 150-155.
- [7] Zhang Faming, Shen Jun, Sun Jianfei, Processing and properties of carbon nanotubes-nano-WC-Co composites, *Materials Science and Engineering A* 2004, 381, 86-91.
- [8] Yaman Bilge, Mandal Hasan, Spark plasma sintering of Co-WC cubic boron nitride composites, *Materials Letters* 2009, 63, 1041-1043.
- [9] Huiyong Rong, Zhijian Peng, Xiaoyong Ren, Chengbiao Wang, Zhiqiang Fu, Longhao Qi, Hezhao Miao, Microstructure and mechanical properties of ultrafine WC-Ni-VC-TaC-cBN cemented carbides fabricated by spark plasma sintering, *Int. J. Refract. Metals Hard Mater.* 2011, 29, 733-738.
- [10] Storms E.K., *The Refractory Carbides*, Academic Press, New York 1967, 3.
- [11] Lipatnikov V.N., Rempel A.A., Gusev A.I., Atomic ordering and hardness of nonstoichiometric titanium carbide, *Int. J. Refract. Met. Hard Mater.* 1997, 15, 61-4.
- [12] Baratti C., Garcia J., Brito P., Pyzalla A.R., Influence of WC replacement by TiC and (Ta,Nb)C on the oxidation resistance of Co-based cemented carbides, *Int. J. Refract. Met. Hard Mater.* 2009, 27, 768-776.